

# Architecture of Optical Fiber Loop for Efficient Optical Buffer and an Ultra-Fast Optical Switching Service

<sup>1</sup>Vivekanand Mishra, <sup>1</sup>Vipin Prasad, <sup>2</sup>Indra Vijay Singh, <sup>1</sup>Rashmi and <sup>3</sup>Vivek Singh

<sup>1</sup>Division of Physics, Department of Science, Alliance University, Bengaluru, Karnataka 562106, India

<sup>2</sup>ICMR Project, Mahatma Gandhi Mission Institute of Health Sciences, Navi Mumbai, Maharashtra 410209, India

<sup>3</sup>Department of Physics, Institute of Science, Banaras Hindu University, Varanasi 221005, India

## ABSTRACT

Optical data storage with fiber loop and ultra-fast optical switching with nonlinear optical loop mirror (NOLM) has been regarded as ideal all-optical processing devices, respectively. The Present article integrates these two devices to provide an efficient buffering-switching device in order to curb signal contention. Various limitations have been analyzed in utilizing the proposed device to obtain an error-free process for the maximum rounds of buffering circulations. The defects evaluated include various types of noises that cause intensity fluctuations in buffered and demultiplexed signals. Switching characteristics of the NOLM demultiplexer were analyzed. The BER vs received optical power with various loop recirculation for the buffering device and signal waveform for NOLM with negligible GVD and walk-off have been calculated. Due to the accumulation of noise from every loop of circulation, the BER increased proportionally with the number of recirculations. However, the simulated results displayed that the input signal is allowed to circulate within the buffer loop of up to one hundred rounds before being demultiplexed by the NOLM switch.

## KEYWORDS

Optical fiber, demultiplexer, ultra-fast and bit error rate, switching service, fiber delay line

*Copyright © 2023 Mishra et al. This is an open-access article distributed under the Creative Commons Attribution License, which permits unrestricted use, distribution and reproduction in any medium, provided the original work is properly cited.*

## INTRODUCTION

Escalating transmission rates in telecommunications networks have prompted widespread localization focalizing in the field of optical communications. Optical signals transmitted directly in the optical layer without resorting to OEO conversion, have emerged as a promising technology for the prolonged advancement of optical networks. Consequently, all-optical processing is crucial for the future of optical communication networks. Due to the inexistence of optical RAM, signal contention is one of the major drawable all-optical communications. Several techniques using fiber delay line (FDL) as storage have been proposed. However, a longer FDL is required for a significant buffering time. Thus, this has prompted the invention of several techniques based on fiber loop recirculation<sup>1-3</sup>, meant for optical buffering purposes. An optical signal is allowed to recirculate within the fiber loop until it is required for transmission. As a



result, the size of the buffer loop is fixed without depending on the length of buffering time required and is much more compact in size as compared to FDL<sup>4</sup>. The NOLM has been proven as an efficient optic DE multiplexer that provides high-speed switching<sup>2,5,6</sup>. In this paper, the proposed combination of optical loop buffer (OLB) with NOLM is utilized to provide efficient matching of the optical buffering-switching device for curbing signal contention. Several types of noises that occur within the proposed device have been taken into consideration in the analysis, in order to obtain the maximum loop circulations for buffering. Besides, several negative effects that take place within the NOLM switch have been analyzed. Among them are the group velocity dispersion (GVD) and pulse walk-off that influenced the transmission and reflection of the signal by the NOLM.

**System model:** The idea of the NOLM demultiplexer has evolved from the Sagnac interferometer. The NOLM is preferred due to its higher switching speed, but lower operating power and simpler setup. In a NOLM demultiplexer, the intensity control signal from the WDM coupler will induce an XPM effect on the clockwise input signal<sup>7</sup>. Thus, it will cause the input signals to experience a refractive index variation due to the Kerr effect. The variation in the refractive index will eventually cause a signal phase shift. Besides, a longer fiber loop is required for constructing the NOLM demultiplexer<sup>8</sup>. This is due to the nonlinear parameter ( $\gamma$ ) for fiber being rather small. Thus, the fiber loop of 3 km is utilized to ensure sufficient power is induced for a phase shift of  $\pi$ . Consequently, the  $\pi$  phase shift between the propagating counter-propagating signals will cause the required portion of the input signal to be transmitted.

In optical communication, all optical buffer device is unavailable. Furthermore, the FDL is impractical to be implemented for the higher buffering period. Hence, the optical loop buffer that has a nearly identical architecture to the NOLM switch suites is ideal for the optical buffering services<sup>9</sup>. It is important to observe that the signal entering the NOLM switch will be split and co-propagate-propagated bi-directionally, while this is not the case for OLB. This is because the NOLM switch requires nonlinear effects, such as XPM, for its switching functions. This also explains the necessity of a longer loop length for NOLM. However, the length of OLB does not depend on the nonlinear index coefficient of the fiber but on the maximum buffer time per loop required. Thus, it is usually more compact. The signals propagating in OLB are not required to split for co-propagation and the inexistence of control signals will be able to avoid extra deficiencies that occurred in NOLM, such as undesired XPM and pulse walk-off. In OLB, the incoming signal is able for multiple recirculation within the OLB until it is required for transmission<sup>10</sup>. The maximum buffer time per loop can be calculated from:

$$T_{\max} = \frac{nl}{c}$$

where,  $n$  is the refractive index of the fiber loop and  $L$  and  $c$  are the loop length and the speed of light respectively. Thus,  $T_{\max}$  for the OLB in the experiment will be 3 microseconds. As a result, a couple of circulations will provide a significant amount of buffer time for the contention resolution. Nevertheless, it is noted that too many circulations may lead to other negative effects.

In view of their respective advantages, the combination of NOLM demultiplexer and OLB will provide an outstanding optical buffering-switching service for the optical networks. The OLB is located before the NOLM switch in order to reduce contention as well as the number of reflected signals by the switch. When the input signal arrives at the switch (Fig. 1), two routes are available for choice. The Input signal that does not require buffering will be switched to the NOLM, without entering the OLB. However, the input signal that needs buffering will be switched into the OLB. The signal that requires a buffer will be switched to the 100:0 coupler before entering the OLB. The main function of this coupler is to couple 100 percent of the signal to the fiber loop through port 3 of the coupler. However, port 4 only allows the signal from the loop to exit. Thus, the signal in the loop will only recirculate in one direction. The optical amplifier in the loop is used to compensate for the losses incurred by the fiber loop and switch. The optical isolator which resembles a diode is utilized to impose one-way traffic for the signal propagating within the loop<sup>11</sup>.

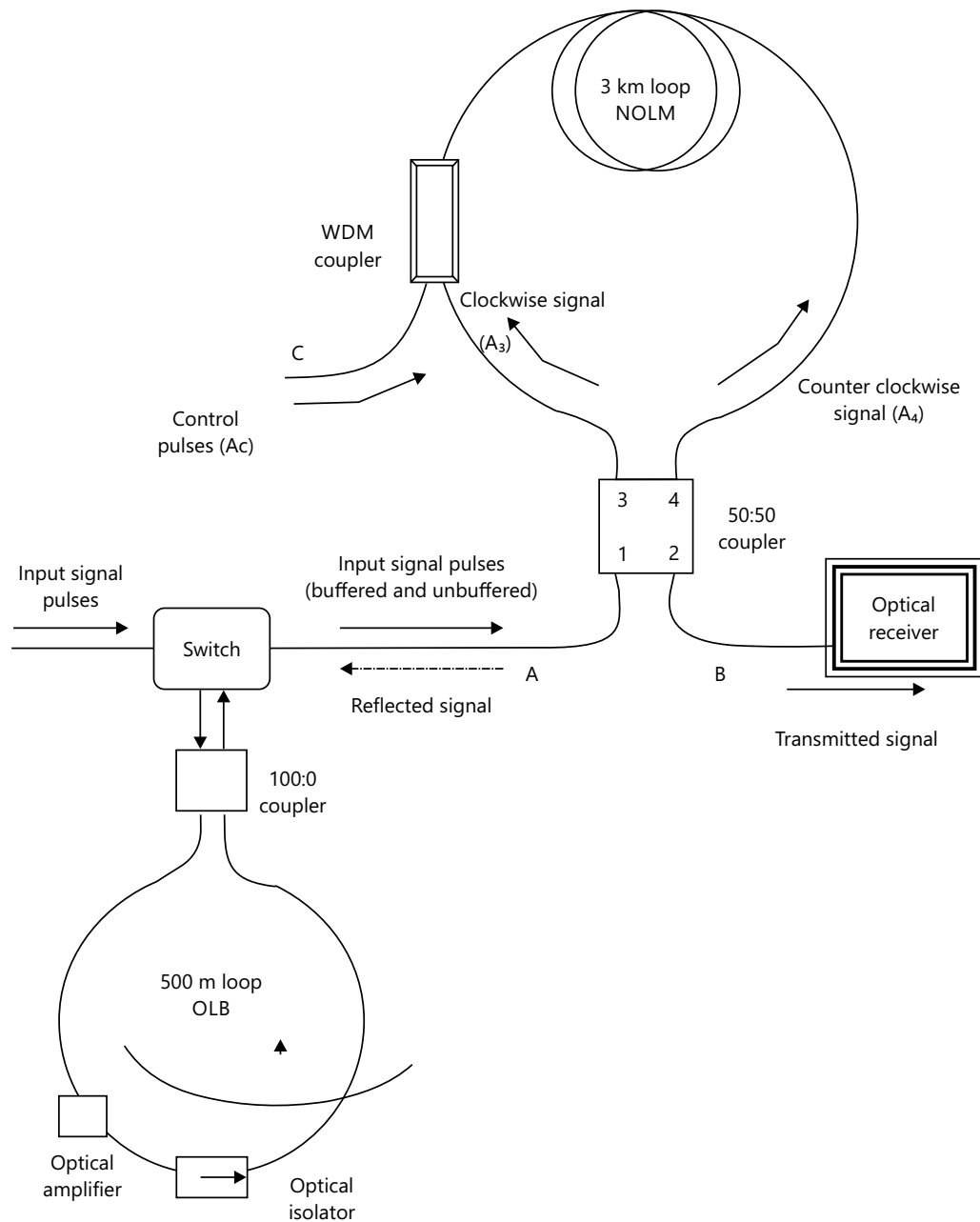


Fig. 1: Schematic diagram of an OLB combined with the NOLM switch (Self-fabricated by Author)

The buffering signal will recirculate within the OLB for a period of time until it is required at the NOLM for transmission. The NOLM demultiplexer in the experiment setup is slightly different from the NOLM switch in<sup>2</sup>, where the semiconductor Optical Amplifier (SOA) is utilized. Thus, the optical nonlinearity of the NOLM switch in this research does not depend on the gain saturation of the SOA, but through the intensity high-intensity control signal induced by the WDM coupler<sup>12</sup>. The control signal will couple with the clockwise signal, thus, causing the signal to undergo a phase shift. Therefore, the phase difference of  $\pi$  between the two counter-propagating signals in NOLM will switch the signal towards the optical receiver.

**Theoretical analysis:** Though the proposed optical buffering and switching device tends to improve the signal throughput of the optical networks, the demultiplexed signal is unavoids from degradation caused by various noise sources. The noises involved are identified as thermal noise, shot noise and several types of beat noise that are related to the spontaneous emission (also can include Amplified Spontaneous Emission (ASE) noise). The OLB allows the signal to recirculate within the fiber loop for a certain number

of rounds. As a result, noises are accumulated for every circulation. The reduced received power at the receiver after the recirculation,  $P_s$  is given by Avramopoulos and Whitaker<sup>13</sup>:

$$P_s = P_N 10^{-z/10} \tag{1}$$

where,  $P_N$  and signifies the output power after N loops of circulations and the amount of data signal attenuation in decibels (dB), respectively. The  $P_s$  will be the input signal power of the buffered signal that enters the NOLM switch. The input signal will be split equally by the 50:50 couplers and co-propagate bi-directionally in the NOLM. The input signal and control pulse are governed by the nonlinear Schrodinger (NLS) equation. The NLS equation is utilized when a long-length fiber is employed, as the dispersive and nonlinear effects are significant in a long fiber. Thus, the signal that propagates in the clockwise, counterclockwise direction and control pulse that satisfies the NLS equation can be written as:

$$\frac{\partial A_3}{\partial z} + \frac{i\beta_{2s}}{2} \frac{\partial^2 A_3}{\partial T^2} = i\gamma_s (|A_3|^2 + 2|A_c|^2) A_3 \tag{2}$$

$$\frac{\partial A_c}{\partial z} + \beta_1 \frac{\partial A_c}{\partial T} + \frac{i\beta_{2c}}{2} \frac{\partial^2 A_c}{\partial T^2} = i\gamma_c (|A_c|^2 + 2|A_3|^2) A_c \tag{3}$$

$$\frac{\partial A_4}{\partial z} + \frac{i\beta_{2s}}{2} \frac{\partial^2 A_4}{\partial T^2} = i\gamma_{sc} |A_4|^2 A_4 \tag{4}$$

where,  $z$  is the distance from port three along the clockwise direction,  $\beta_{2s}$  and  $\beta_{2c}$  are the GVD parameters for signal and control pulse, respectively,  $T$  is the time variable in retarded frame,  $\gamma_s$  and  $\gamma_c$  are the nonlinear coefficient parameter of signal pulse and control pulse, respectively<sup>13</sup>.

Besides, the signal pulse in the clockwise direction ( $A_3$ ), counterclockwise direction ( $A_4$ ) and the control pulse ( $A_c$ ) are listed as follows:

$$A_3 = (1-K)^{1/2} (P_1)^{1/2} (P_0)^{1/2} e^{-t^2/2} (T_{01})^4 \tag{5}$$

$$A_4 = j(K)^{1/2} (P_1)^{1/2} (P_0)^{1/2} e^{-t^2/2} (T_{01})^4 \tag{6}$$

$$A_c = (P_2)^{1/2} (P_0)^{1/2} e^{-t^2/2} (T_{02})^4 \tag{7}$$

where,  $K$  represents the coupling ratio,  $P_1$  and  $P_2$  are the peak power for the signal pulse and control pulse respectively,  $P_0$  is the input power,  $t$  is the time variable,  $T_{01}$  corresponds to the full width at half maximum (FWHM) for the signal pulse<sup>14</sup>.

The control pulse from WDM coupler will couple and co-propagate with the desired section of the clockwise propagating signal that is required for transmission. The signal pulse that is transmitted out of the fiber loop is written as:

$$\text{Signal out} = (1-K)^{1/2} E_4 + j(K)^{1/2} E_1 \tag{8}$$

where,  $E_1$  and  $E_4$  represent the clockwise and counterclockwise propagating signals, respectively. The values of  $E_1$  and  $E_4$  are calculated numerically by using the split-step Fourier Method (SSFM)<sup>8</sup>.

However, without any control pulse coupled into the fiber loop, both clockwise and counterclockwise propagating signals will not experience any phase difference. Therefore, the input signal will be reflected back after propagating along the loop. The reflected signal pulse is given by:

$$\text{Signal reflect} = j(K)^{1/2} E_4 + j(1-K)^{1/2} E_1 \quad (9)$$

Thus, the Transmittance ( $\nu$ ) of the NOLM demultiplexer can be obtained from:

$$\nu = \frac{|\text{signal\_out}|^2}{|\text{signal\_input}|^2} \quad (10)$$

The bit error rate (BER) analysis is utilized to evaluate the signal degradation related to NOLM demultiplexing. The variance of thermal noise and shot noise can be obtained from<sup>8</sup>:

$$\sigma_{th}^2 = \frac{4kTB}{R_L} \quad (11)$$

$$\sigma_{sh,a}^2 = 2qI_r B \quad (12)$$

where,  $k$  and  $q$  have fixed values, representing Boltzmann's Constant and electron charge, respectively,  $T$  indicates the temperature,  $B$  is electrical bandwidth,  $R_L$  is load resistance of the photodiode,  $I_r$  is the photocurrent generated at the receiver. For signals 0 and 1,  $I_r$  becomes  $I_0$  and  $I_1$ , respectively. Furthermore, several types of spontaneous beat noise related to the preamplifier, such as beat noise between signal and spontaneous emission, spontaneous emission against itself and shot noise against spontaneous emission have caused some deficiencies in the output signals. The beating between the signal and spontaneous emission is due to both having different optical frequencies. However, the inter-beating between the spontaneous emissions occurs as it extends over a wide frequency range that is governed by its effective bandwidth<sup>3,8-10</sup>. Therefore, current fluctuations due to the inter-beatings have generated the beat noise that causes signal degradation. For the NOLM operations, the variances of beat noise discussed above are as follows:

$$\sigma_{sg\_spn,r}^2 = 4R^2 G_p S_{sp} \overline{BN}_r \quad (13)$$

$$\sigma_{sg\_spn}^2 = 4R^2 S_{sp} fB \quad (14)$$

$$\sigma_{sh\_spn}^2 = 4qRS_{sp} fB \quad (15)$$

where,  $f$  is the receiver optical bandwidth and the spontaneous emission noise spectral density ( $S_{sp}$ ) is given by:

$$S_{sp} = (G-1)n_{sp} hf \quad (16)$$

where,  $G$  and  $h$  signify the optical amplifier gain and Planck's constant respectively and  $n_{sp}$  is the spontaneous emission factor. The mean photon number ( $\overline{N}_r$ ) for signal 0 and 1 will become  $\overline{N}_0$  and  $N_1$ , respectively. Both the value of  $I_r$  and  $\overline{N}_r$  have been assessed with the GVD, pulse walk-off between signal and control pulse, channel and intrinsic crosstalk effects on the demultiplexed signals. Channel crosstalk

is defined as the undesired channel that has been switched to the output port during demultiplexing and it is due to the switching window that overlaps into the adjacent signal pulses. Meanwhile, intrinsic crosstalk is identified as a small amount of leakage signal at the output, even without any control signal present in the NOLM. Thus,  $\bar{N}_0$  and  $N_1$  of the demultiplexed signals are given by:

$$\bar{N}_1 = \bar{N}_s [1 + CX(F_{TDM} - 1)(R_1 + E_r + E_r R_1)] \tag{17}$$

$$\bar{N}_0 = \bar{N}_s [E_r + CX(F_{TDM} - 1)(R_1 + E_r + E_r R_1)] \tag{18}$$

where,  $F_{TDM}$  is the TDM factor,  $R_1$  is the signal's mark ratio,  $E_r$  is the intensity modulator's extinction ratio in the optical transmitter,  $\bar{N}_s$  represents the mean photon number when only the "1" bits present,  $CX$  is the channel crosstalk,  $CX$  is related to intrinsic crosstalk ( $IX$ ) and can be written as<sup>10,11</sup>:

$$CX = 1 - (1 - IX) \cos \left[ \frac{\pi}{2(E - 1)} \right]^2 \tag{19}$$

Where:

$$E = \frac{1}{f_c \beta_1} \operatorname{erf} \left( \frac{\beta_1 \sqrt{\ln 2}}{T_{02}} \right) \tag{20}$$

where,  $T_{02}$  corresponds to the Full Width at Half Maximum (FWHM) for the control pulse,  $\beta_1$  represent the walk-off parameter,  $f_c$  is the control pulse repetition rate. Besides, due to intensity fluctuation caused by the timing jitter between control and input signal, the relative intensity noise variance for signal 0 and 1 will be included into the analysis of NOLM demultiplexer and is given by:

$$\sigma_{RIN_0}^2 = (q\eta G_p)^2 \left[ RIN(\bar{N}_0)^2 B + RIN_{NOLM}(E_r)^2 (\bar{N}_s)^2 \right] \tag{21}$$

$$\sigma_{RIN_1}^2 = (q\eta G_p)^2 \left[ RIN(\bar{N}_1)^2 B + RIN_{NOLM}(\bar{N}_s)^2 \right] \tag{22}$$

where,  $\eta$  represents the photodetector quantum efficiency,  $RIN$  and  $RIN_{NOLM}$  signify the relative intensity noise of the optical signal source and intensity fluctuation due to NOLM demultiplexing, respectively. As a result, the variance of the current fluctuation for the NOLM switch can be written as:

$$\sigma_q^2 = \sigma_{th}^2 + \sigma_{sh_a}^2 + \sigma_{sg\_spn\_r}^2 + \sigma_{spn\_spn}^2 + \sigma_{sh\_spn}^2 + \sigma_{RIN_0}^2 + \sigma_{RIN_1}^2 \tag{23}$$

For signals 0 and 1 in the NOLM analysis,  $\sigma_q^2$  in Eq. 23 will be replaced with  $\sigma_0^2$  and  $\sigma_1^2$ , respectively. To evaluate signals undergone the optical buffering and switching devices, the bit error rate (BER) used will be given as:

$$BER = \frac{1}{2} \operatorname{erfc} \left[ \frac{I_1}{\sqrt{2}(\sigma_1 + \sigma_0)} \right] \tag{24}$$

where,  $I_1 = RP_{1a}$  and  $P_{1a}$  represents the output power from the switch.

**RESULTS AND DISCUSSION**

To date, a variety of optical storage elements have been demonstrated<sup>10</sup>. Most promising for slotted TDM applications are the regenerative buffers employing optical logic gates<sup>10-13</sup> and the compensating fiber loops buffers<sup>13-18</sup>. These two types of buffers are attractive from a network standpoint because they can be designed to store a single packet at a single wavelength for hundreds of circulations. Because of the cyclical nature of the memory, reading of the information is restricted to multiples of the round trip loop time (packet length)<sup>19</sup>.

Ultra-fast optical switching with nonlinear optical loop mirror (NOLM). Numerical analysis is performed to achieve an error-free optical buffering-switching service with the system model as illustrated in Fig. 1. The primary objective of the two results depicted below are to obtain the maximum rounds of recirculation for the data packets with 512 bits per packet. Figure 2 demonstrated the BER analysis of the buffered signal after various loop recirculation’s within the OLB. Next, Fig. 3 illustrated the BER analysis for the buffered signal that has been demultiplexed by the NOLM switch. Both experiments are based on the parameters as follows: Data rate is 10 Gbps:

$$E_r = -25, \eta = 0.7, T = 293 \text{ K}, f = 374 \text{ Ghz}, B = \frac{1}{2} (\text{data rate}), R = 0.9, \text{RIN} = 10^{-15}, \text{RIN}_{\text{NOLM}} = 1^{-3}, T_0 = 5^{-12}$$

In Fig. 2, input signal that experienced 20 circulation buffer outperformed the other experiments with higher loop circulations. The higher the number of circulations, the BER will deteriorate further. This phenomenon mainly attributes to the intensity fluctuation of the signal caused by various sources of noise as discussed above. According to, one hundred loops circulation within the OLB will offer approximately three hundred microseconds of optical buffering time and it is still able to achieve an error-free process.

When the signal is required for transmission, it will propagate towards the NOLM demultiplexer. The buffered signal will undergo an ultra-fast nonlinear switching process. Figure 3 depicted the BER analysis for various numbers of loop buffering signals that experience NOLM demultiplexing when data rate equals to 10 Gbps. Figure 4 illustrates the BER analysis when the data rate is increased to 20 Gbps. It is noted that the BER performance deteriorates with higher data rate. The simulated result for the demultiplexed signal demonstrated a significant decline in the BER performance as compared to BER analysis in Fig. 2.

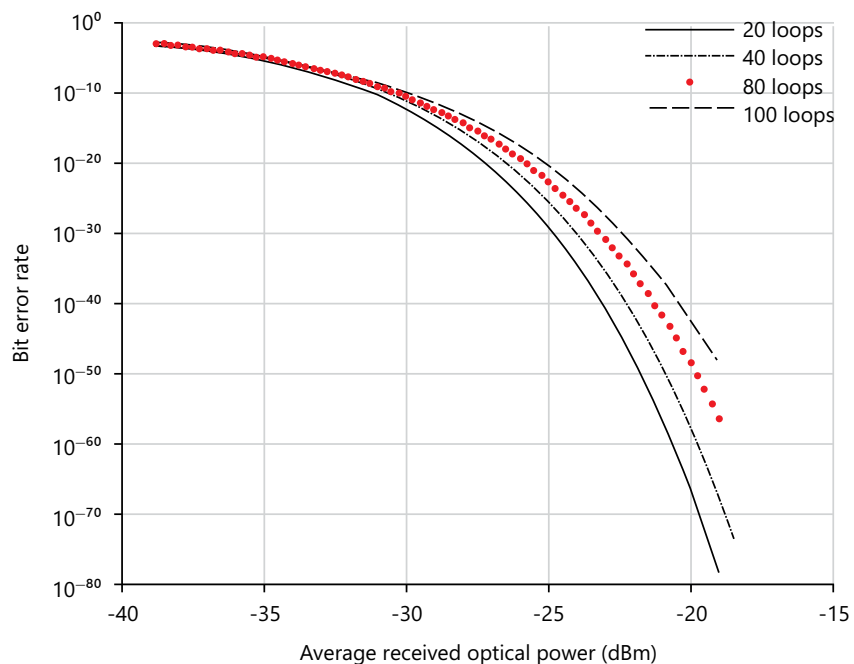


Fig. 2: BER vs received optical power with various loop recirculation for the buffering device

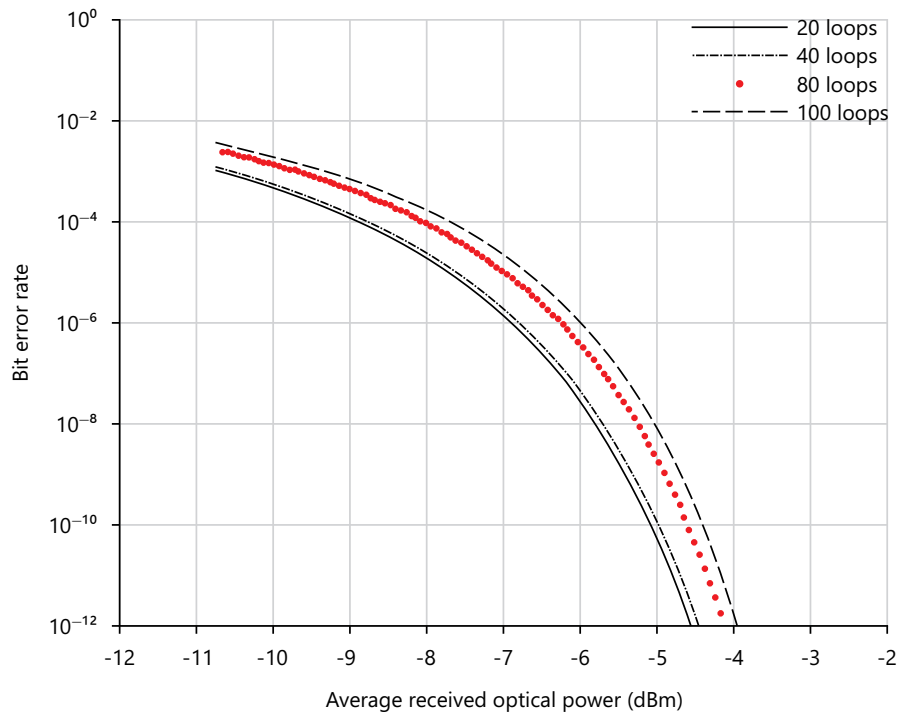


Fig. 3: BER vs received optical power with various loop recirculation for the buffering device and demultiplexing by NOLM when data rate equals 10 Gbps

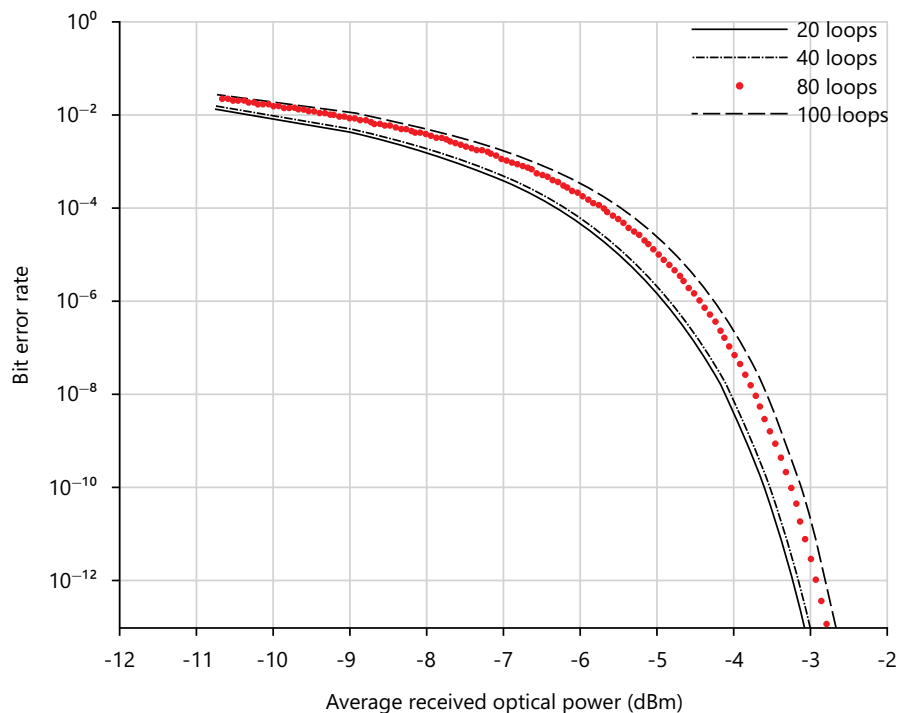


Fig. 4: BER vs received optical power with various loop recirculation for the buffering device and demultiplexing by NOLM when data rate equals 20 Gbps

This circumstance attributes to the various noise sources that have been experienced in OLB, in addition to a number of nonlinear related effects. The negative effects are identified as GVD, pulse walk-off, channel and intrinsic crosstalk<sup>13</sup>. However, the result shows that signals propagating through the proposed model are still allowed for up to a hundred loop circulations and are within the reasonable received optical power range.

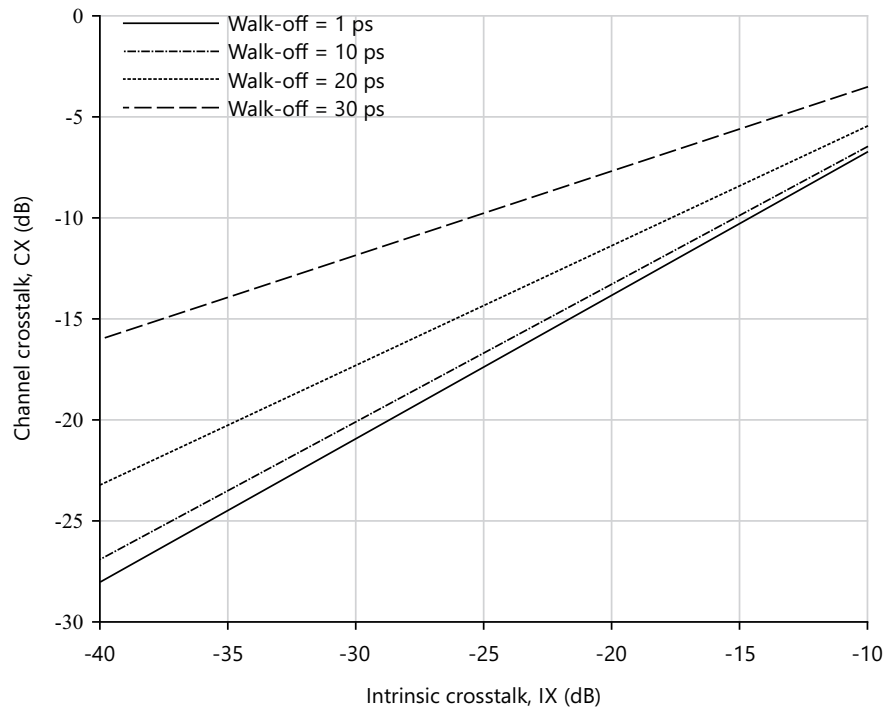


Fig. 5: Channel crosstalk vs intrinsic crosstalk for various value of pulse walk-off

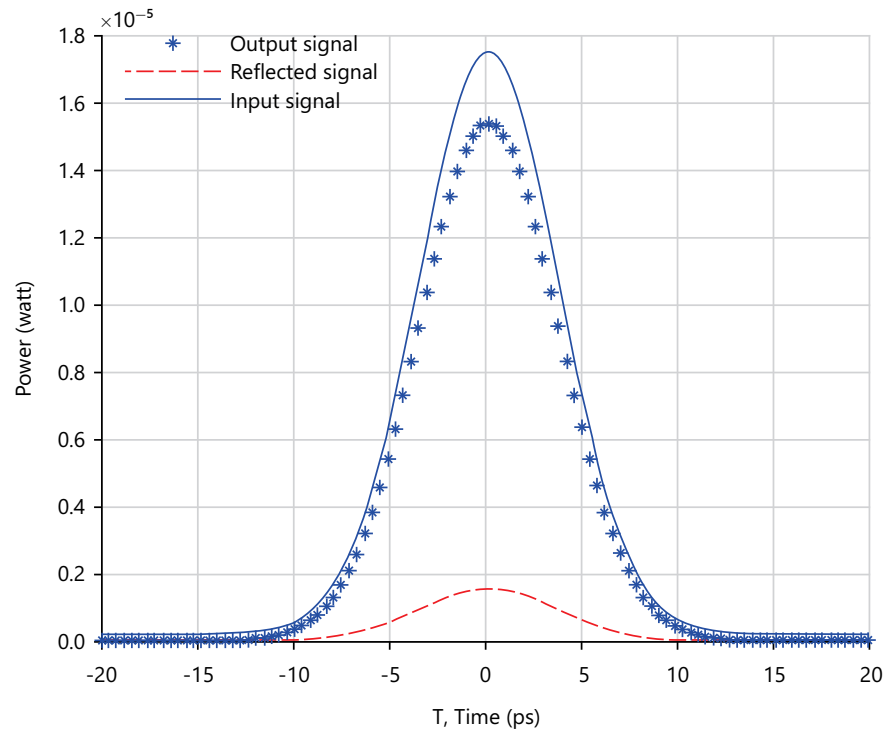


Fig. 6: Signal waveform for NOLM with negligible GVD and walk-off

The simulated result illustrates the inter-relationship between channel and intrinsic crosstalk with various value of pulse walk-off between control and input signal. It can be observed that higher walk-off will increase the minimum value of channel crosstalk with respect to the intrinsic crosstalk as shown in Fig. 5. Thus, this has proven that pulse walk-off will raise the channel crosstalk affecting the demultiplexed signals.

Several unchanged parameters utilized in Fig. 6 and 7 are as follows:

$$K = 0.5, T_{01} = 3\text{ps}, T_{02} = 4\text{ps}$$

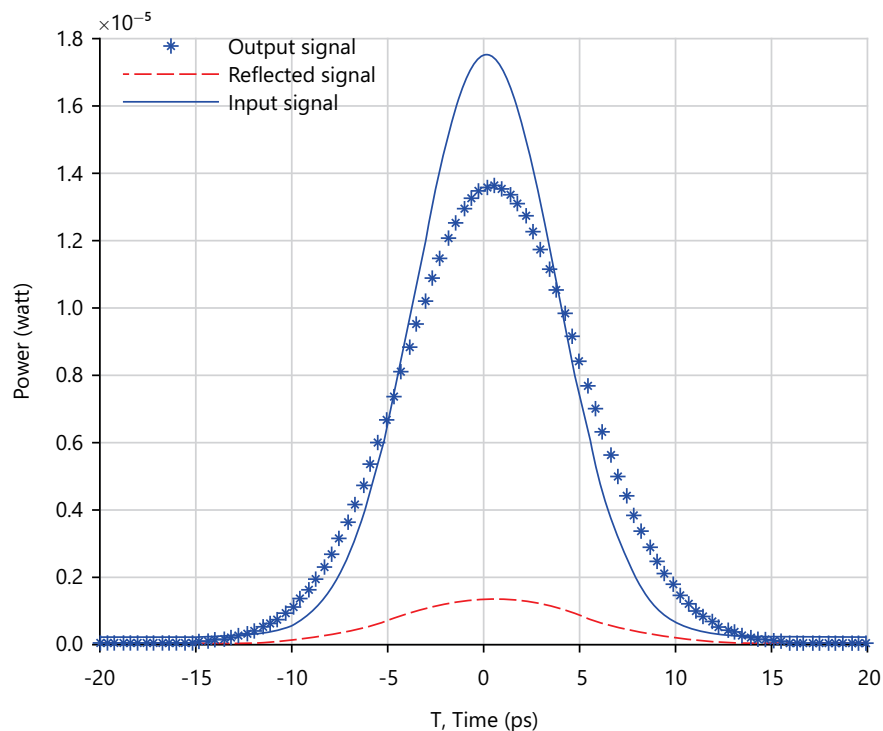


Fig. 7: Signal waveform for NOLM with more significant GVD and walk-off

Figure 6 illustrates the signal waveform propagating in the NOLM switch with negligible value of GVD and pulse walk-off. The signals are concentrated within the switching profile. However, practical NOLM switch involves higher value of GVD and pulse walk-off that causes the signals to broaden and swerve from the middle position, as depicted in Fig. 7. This occurrence has degraded the switching efficiency, thus, deteriorates the BER performance (Fig. 3).

## CONCLUSION

A new optical buffering-switching device has been proposed in this paper. The device is designed using the optical fiber loop architecture to provide a compact but efficient optical buffer and an ultra-fast optical switching service. The simulated results have revealed that signal propagating through both fiber loops suffered intensity fluctuations due to various sources of noise. Moreover, GVD, pulse walk-off, channel and intrinsic crosstalk occurs during NOLM demultiplexing have further deteriorate the data signal. GVD and pulse walk-off are the major contributors of pulse broadening and deviation for the signal propagating in NOLM. Pulse walk-off also increases the channel crosstalk that deteriorates the demultiplexed signals. Due to the accumulation of noise from every loop of circulation, the BER increased proportionally with the number of recirculation. However, the simulated results displayed that the input signal is allowed to circulate within the buffer loop of up to one hundred rounds before being demultiplexed by the NOLM switch.

## SIGNIFICANCE STATEMENT

This study discovered the novel buffering structure where more than one packet can be stored in single fiber delay line with a single amplifier. That can be beneficial for large storage of capacity. This study will help the researchers to uncover the critical areas of ultra-fast optical switching with nonlinear optical loop mirror (NOLM) that many researchers were not able to explore. Thus a new theory on Ultra-Fast Optical Switching Service may arrive at WDM technology.

## REFERENCES

1. Bogris, A., 2018. An all-optical buffer based on non-degenerate phase-sensitive parametric amplification. *J. Lightwave Technol.*, 36: 5949-5955.
2. Tang, M.F., F.M. Abbou, A. Abid, V.N. Mishra and H.T. Chuah, 2006. Packet loss rate of an optical burst switch with nonlinear optical loop mirrors. *IEICE Electron. Express*, 3: 243-248.
3. Agrawal, G.P., 1997. *Fiber-Optic Communication Systems*. 2nd Edn., Wiley, New York, ISBN: 9780471175407, Pages: 576.
4. Grendar, D., O. Pottiez, M. Dado, J. Müllerová and J. Dubovan, 2009. Effect of control-beam polarization and power on optical time-domain demultiplexing in a new nonlinear optical loop mirror design. *Opt. Eng.*, Vol. 48. 10.1117/1.3125427.
5. Bogoni, A., M. Scaffardi, P. Ghelfi and L. Poti, 2004. Nonlinear optical loop mirrors: Investigation solution and experimental validation for undesirable counterpropagating effects in all-optical signal processing. *IEEE J. Select. Topics Quantum Electron.*, 10: 1115-1123.
6. Sakamoto, T., F. Futami, K. Kikuchi, S. Takeda, Y. Sugaya and S. Watanabe, 2001. All-optical wavelength conversion of 500-fs pulse trains by using a nonlinear-optical loop mirror composed of a highly nonlinear DSF. *IEEE Photon. Technol. Lett.*, 13: 502-504.
7. Huang, T., J. Li, J. Sun and L.R. Chen, 2011. Photonic generation of UWB pulses using a nonlinear optical loop mirror and its distribution over a fiber link. *IEEE Photon. Technol. Lett.*, 23: 1255-1257.
8. Bogoni, A., P. Ghelfi, M. Scaffardi and L. Poti, 2004. All-optical regeneration and demultiplexing for 160-Gb/s transmission systems using a NOLM-based three-stage scheme. *IEEE J. Select. Topics Quantum Electron.*, 10: 192-196.
9. Leuthold, J., C. Koos and W. Freude, 2010. Nonlinear silicon photonics. *Nat. Photonics*, 4: 535-544.
10. Gautam, A.K. and V. Mishra, 2011. Modelling dispersion characteristics of circular optical waveguide with helical winding-comparison for different pitch angles. *Int. J. Opt. Photonics*, 5: 35-40.
11. Abd-Rahman, F., P.K. Choudhury, D. Kumar and Z. Yusoff, 2009. An analytical investigation of four-layer dielectric optical fibers with an nano-coating-a comparison with three-layer optical fibers. *Prog. Electromagn. Res.*, 90: 269-286.
12. Hall, K.L. and K.A. Rauschenbach, 1998. 100-Gbit/s bitwise logic. *Opt. Lett.*, 23: 1271-1273.
13. Avramopoulos, H. and N.A. Whitaker, 1993. Addressable fiber-loop memory. *Opt. Lett.*, 18: 22-24.
14. Whitaker, N.A., M.C. Gabriel, H. Avramopoulos and A. Huang, 1991. All-optical, all-fiber circulating shift register with an inverter. *Opt. Lett.*, 16: 1999-2001.
15. Poustie, A.J., R.J. Manning and K.J. Blow, 1996. All-optical circulating shift register using a semiconductor optical amplifier in a fibre loop mirror. *Electron. Lett.*, 32: 1215-1216.
16. Hall, K.L., J.P. Donnelly, S.H. Groves, C.I. Fennelly, R.J. Bailey and A. Napoleone, 1997. 40-Gbit/s all-optical circulating shift register with an inverter. *Opt. Lett.*, 22: 1479-1481.
17. Doerr, C.R., W.S. Wong, H.A. Haus and E.P. Ippen, 1994. Additive-pulse mode-locking/limiting storage ring. *Opt. Lett.*, 19: 1747-1749.
18. Moores, J.D., K.L. Hall, S.M. LePage, K.A. Rauschenbach, W.S. Wong, H.A. Haus and E.P. Ippen, 1995. 20-GHz optical storage loop/laser using amplitude modulation, filtering, and artificial fast saturable absorption. *IEEE Photon. Technol. Lett.*, 7: 1096-1098.
19. Hall, K.L., J.D. Moores, K.A. Rauschenbach, W.S. Wong, E.P. Ippen and H.A. Haus, 1995. All-optical storage of a 1.25 kb packet at 10 Gb/s. *IEEE Photon. Technol. Lett.*, 7: 1093-1095.